A TWIN-CLUSTER MIMO CHANNEL MODEL

Helmut Hofstetter[1], **Andreas F. Molisch**[2,3], **and Nicolai Czink**[4,5]

[1]*Eurecom Institute, Sophia Antipolis, France*
[2]*Mitsubishi Electric Research Laboratories (MERL), Cambridge, MA, USA*
[3]*Lund University, Lund, Sweden*
[4]*Institut für Nachrichtentechnik und Hochfrequenztechnik, Technische Universität Wien, Vienna, Austria*
[5]*Forschungszentrum Telekommunikation Wien (ftw.), Vienna, Austria*

ABSTRACT

The paper presents a new approach to geometry-based stochastic channel models that can be used for simulating MIMO systems. We use twin-clusters to represent multiply reflected or diffracted multipath components. The location of the two twins can be chosen independently, in order to correctly reflect DoAs, DoDs, and delays. The model is thus more accurate than existing single-scatterer approaches. Simulation results, using a publicly available version of our model, show a very realistic behavior of our model.

1. INTRODUCTION

MIMO (multiple-input - multiple-output) systems have emerged as one of the most promising approaches for high-data rate wireless systems [1], [2]. In principle, the information-theoretic capacity of these systems can increase linearly with the number of antennas. In order to achieve or at least approach those capacities, sophisticated signal processing algorithms (like BLAST [3]) and coding strategies [4] have been developed, and research on those topics continues. Furthermore, MIMO systems are now being introduced into standardized systems, including the IEEE 802.11n standard for high-throughput wireless local area networks [5], and the long-term evolution (LTE) of the third-generation cellular standard 3GPP, as well as for metropolitan area networks like IEEE 802.16 (WiMax).

In order to design MIMO systems and assess their performance, realistic channel models that are suitable for multi-antenna systems are required. Due to the high importance of this topic, a lot of effort by the channel modelling community has been spent on this, and two types of channel models have emerged: models that describe the transfer function between the antenna elements, and so-called "double-directional models" [6], which describe the directions-of-arrival and directions-of-departure of the multipath components (MPCs) in the channel. The latter models are especially suitable for system design, because they allow to analyze the impact of different antenna arrangements, channel changes by the presence of a user, etc.

In general, there are three generic approaches for channel modelling [7] (i) stochastic models, (ii) deterministic (ray-tracing) based models, and (iii) geometry-based stochastic models (GSCMs). GSCMs are an efficient and natural way to simulate propagation channels: the location of scatterers and other interacting objects is placed at random, according to a certain probability distribution; during the simulation, the propagation of the MPCs from the transmitter to the receiver is then traced. GSCMs have been used for the simulation of systems with receive diversity antennas since the 1970s [8], and developed in more detail in [9], [10], [11] A more general, cluster-based model was introduced in [12]. Ref.[13] also includes the Doppler effect. The GSCM was also suggested as one method for implementing the standardized COST 259 channel model [14].

The GSCM papers mentioned above are based on the assumption that MPCs undergo only single-interaction processes on the way from the transmitter to the receiver. Even in those cases where an MPC undergoes multiple interaction processes, all those processes could be represented adequately by "equivalent" single-interaction processes. If there are multiple antennas only at one link end, then it is always possible to describe the properties of an MPC (delay, angle-of-arrival) by an "equivalent interacting object (IO)". In other words, we can always place an IO in such a way that a single-interacting process leads to the desired delay and angle-of-arrival[15]. However, such an equivalent representation is not possible in MIMO systems. A number of attempts have been made at generalizing GSCMs to the MIMO case. [16] suggested a two-ring model (scatterers placed near the BS, and near the MS) that explicitly models double-interaction processes, and allows an explanation of the so-called "keyhole" effect. [17] gave a comprehensive model that included single- and double-interactions, as well as wave guiding and other effects; however, the large number of parameters makes this model difficult to parameterize from measurements.

In this paper, we propose a new approach that is based on the concept of "twin clusters". In essence, we geometri-

cally place two closely coupled clusters of IOs. MPCs originate from the transmitter, travel from there to the first cluster, are transferred to a corresponding IO in the "twin cluster", and from there to the receiver. The position of the clusters is chosen in such a way that both the directions-of-departure and the directions-of-arrival are reproduced correctly; the transferring between the two clusters adds a delay that also matches the measured delay of the MPCs. Thus, the method is capable of producing any desired DOA/DOD/delay distribution of the MPCs; furthermore, the method is very computationally efficient. For this reason, it has also been adopted as a fundamental modelling approach for the COST 273 standardized model, [18]. For the parametrization of our model angular and delay statistics of the MPCs are required. [19] and [20] propose a methodology of analyzing measurements based on clusters and MPCs. These statistics can be used for the parametrization of our model.

The remainder of the paper is organized the following way. Section 2 describes the basic model structure, followed by a discussion on the visibility of clusters due to the movement of the MT. The intra cluster power weighting and distribution of the MPCs is discussed in Section 4. In Section 5 we give a reference on the source code of our model which we used for deriving all of our results described in Section 6. Finally concluding remarks are made in Section 7.

2. MODEL STRUCTURE

In geometry-based stochastic channel models, it is assumed that each wave is reflected or diffracted at an interacting object (IO) and propagated towards the receiver. IOs are usually grouped into clusters, corresponding, e.g., to groups of buildings or objects in a room. In contrast to ray-tracing models the IOs are placed in accordance to stochastic distributions and not real world scenarios (maps). We have chosen a set of nine parameters that describe the propagation properties of a single path including polarization. The parameters are given in Table 1.
The paths are defined as they are observed by the antennas. From the Tx antenna towards the first interaction and from the last IO towards the Rx antenna. There is no difference between single-bounce and multiple-bounce paths.

The impulse response can be written as the sum of all the MPCs

$$\begin{aligned}\mathcal{H}(\tau,\theta_{DoA},\theta_{DoD},\phi_{DoA},\phi_{DoD}) = \\ \sum_{s=1}^{S}\Gamma_s\delta(\tau-\tau_s)\delta(\theta-\theta_{DoD,s})\delta(\theta-\theta_{DoA,s}) \\ \delta(\phi-\phi_{DoD,s})\delta(\phi-\phi_{DoA,s}),\end{aligned} \quad (1)$$

where S denotes the number of paths, $\mathcal{H}$ keeps the impulse responses of all four main polarization combinations

$$\mathcal{H} = \begin{bmatrix} h_{VV} & h_{VH} \\ h_{HV} & h_{HH} \end{bmatrix}, \quad (2)$$

and Γ is the polarization matrix of the attenuation coefficients

$$\Gamma_s = \begin{bmatrix} A_{VV,s} & A_{VH,s} \\ A_{HV,s} & A_{HH,s} \end{bmatrix}. \quad (3)$$

The elements of Γ are typically complex valued allowing for independent phase shifts of polarization components of each path. Note that all the parameters are time-dependent. To keep the formula readable the time-index is omitted for all the parameters.

The detailed properties of the antennas remain unspecified at this point. The directivity and orientation of the antennas will have strong influence on the radio channel. In the simplest case of omni-directional antennas at both sides, $\mathcal{H}$ simplifies to h_{VV} and all the other parameters can be neglected since none of the antennas can *'see'* the corresponding contributions. For this paper we will restrict ourselves to the vertical-to-vertical polarization component only. An extension to the dual polarized cased can be found in [21]. The polarization matrix Γ is therefore reduced to $A_{VV,s}$ which will be called A_s in the following for simplicity.

In single-bounce geometry-based models, it is assumed that there is only interaction with one IO for each wave [22], [23], [24]. Such models are well suited for smart antenna systems with an antenna array only at one link end. Due to the geometrical placement of objects in space the relation between DoD, delay and DoA is given by a triangulation. Only two out of these three parameters can be chosen, the third one is derived from the geometry. In MIMO systems, however, this is approach is insufficient[1]. To avoid the limitations of single-interacting clusters researchers have started to include double-bounce paths in their models [25]. Each path interacts at an IO related to the transmitter and an IO related to the receiver. The increase in complexity of such a model is tremendous. For a set of S_N objects at the transmitter and S_M objects at the receiver the total number of paths S, which have to be evaluated, is the product of both values

$$S = S_N S_M. \quad (4)$$

To overcome this limitation, we introduce the concept of twin-clusters in COST 273. One cluster is split up into two representations of itself: one that represents the cluster as seen by the BS and one as it is seen by the mobile terminal (MT) (Figure 1). The two representations are linked via a stochastic cluster link delay $\tau_{\text{C,link}}$ which is the same for all IOs inside a cluster. The cluster link delay ensures realistic path delays as, for example, derived from measurement campaigns, whereas the placement of the clusters is driven by the angular statistics of the cluster as observed from BS/MT respectively. Note that this

[1]Geometry-based channel models show an abstract illustration of measured scenarios and the obtained parameters. Measured parameters are quantized to pdfs and these pdfs are taken to generate single realizations for the model. Even, if in real life the propagation is dominated via single bounce MPCs, it cannot be assured that the mapping of clusters based on individual statistics of delay, DoD, and DoD gives meaningful results. Joint statistics of these three parameters would be necessary to model an environment dominated by single-bounce MPCs via single interacting objects only.

approach is different from any multi-bounce model [26] since the twin-cluster is only one cluster having a defined shape and placement of IOs inside the cluster. It is placed twice on the map and both realizations look identical, like twins. Each ray propagated at the transmitter is bounced at each IO in the corresponding cluster and reradiated at the same IO of the twin cluster towards the receiver. In between the two representations of the cluster only the cluster link delay is added which is the same for all MPCs of a cluster. The shape of the cluster is an ellipsoid where the sizes of the main axes are defined by the delay spread and the angular spread in azimuth and elevation. Due to different angular spreads at MT and BS the cluster at the MT might become a scaled version of the BS cluster. Such a scaling applies on the positions of the IOs as well. Furthermore each IO at the BS-side cluster has exactly one counterpart at the MT-side. Therefore the total number of multipath components is equal to the number of IOs. The distribution of IOs within a cluster is discussed in Section 4.

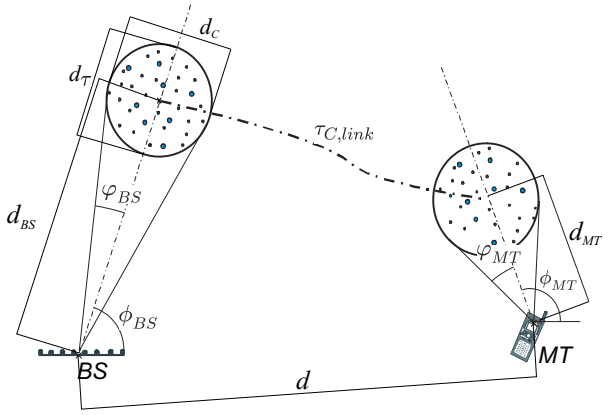

Figure 1. The Twin-cluster concept.

In the following the concept of how to model a cluster based on above assumptions is developed. The large-scale behavior is an essential part of the model. All components of the model are placed on a map covering the simulation environment. This facilitates to model the movement of MTs and clusters compared to an approach in the delay-azimuth plane.

In a first step the start positions of the BS and MT are assigned (Figure 1). The spreads $\varphi_{\text{BS/MT}}$ and directions $\phi_{\text{BS/MT}}$ of a cluster in azimuth are assigned at random from the corresponding distribution functions

$$\phi_{\text{BS}} = \mathcal{F}(\Phi_{\text{BS}}), \tag{5a}$$
$$\phi_{\text{MT}} = \mathcal{F}(\Phi_{\text{MT}}), \tag{5b}$$
$$\varphi_{\text{BS}} = \mathcal{F}(\Phi_{\text{BS}}), \tag{5c}$$
$$\varphi_{\text{MT}} = \mathcal{F}(\Phi_{\text{MT}}). \tag{5d}$$

The distance of the cluster from BS or MT are given as a stochastic parameter $d_{\text{BS}} = \mathcal{F}(D_{\text{BS}})$ and $d_{\text{MT}} = \mathcal{F}(D_{\text{MT}})$(Figure 1). If this parameter is not available we use the following geometric approach. The goal is to get a circular cluster shape in the azimuth-delay plane. The size of the cluster in delay direction d_τ(following the line away from the BS/MT) and the size in azimuth direction d_{C} are by definition the same: $d_{\text{C}} = d_\tau$. The position of the cluster in space is therefore computed by

$$d_{\text{BS}} = \frac{d_\tau}{2\tan(\varphi_{\text{BS}})}, \tag{6a}$$
$$d_{\text{MT}} = \frac{d_\tau}{2\tan(\varphi_{\text{MT}})}, \tag{6b}$$

where $d_\tau = \frac{1}{2}\tau c_0$. Note that the parametrization is not based on any physical argument. The size of the cluster in elevation is now straight forward using the angular spread in elevation

$$\vartheta_{\text{BS}} = \mathcal{F}(\Theta_{\text{BS}}), \tag{7a}$$
$$\vartheta_{\text{MT}} = \mathcal{F}(\Theta_{\text{MT}}), \tag{7b}$$

of the cluster. Geometrical considerations lead to

$$h_{\text{C}}^{\text{BS}} = d_{\text{BS}} \tan\vartheta_{\text{BS}}, \tag{8a}$$
$$h_{\text{C}}^{\text{MT}} = d_{\text{MT}} \tan\vartheta_{\text{MT}}. \tag{8b}$$

The angular directions of the cluster in elevation

$$\theta_{\text{BS}} = \mathcal{F}(\Theta_{\text{BS}}), \tag{9a}$$
$$\theta_{\text{MT}} = \mathcal{F}(\Theta_{\text{MT}}), \tag{9b}$$

are now obtained from their corresponding distribution functions as the last step to fix the cluster in space.

Note also that if talking about spreads and the resulting dimensions of clusters, we always mean the σ-RMS spread. A cluster should cover an area of about 3σ for simulations. Figure 1 shows the cluster definition for the 2-dimensional case. Note that the spreading of the cluster can be represented either in the geometrical plane (like in Figure 1), or in the delay-azimuth plane. It is obvious that the position of a cluster as seen from the BS is not the same as it is seen from the MT. An additional cluster link delay $\tau_{\text{C,link}}$ is introduced, which ensures that the total delay of the cluster τ_{C} corresponds to the definitions of the scenario

$$\tau_{\text{C}} = \tau_{\text{C,BS}} + \tau_{\text{C,link}} + \tau_{\text{C,MT}}, \tag{10}$$

where τ_{C} is obtained from the cluster delay pdf $\mathcal{F}(\tau_{\text{C}})$ which is an exponentially declining function [27]. The cluster link delay $\tau_{\text{C,link}}$ is calculated once when the cluster is placed. It may happen that this cluster link delay $\tau_{\text{C,link}}$ of a cluster becomes negative. A negative link delay occurs if the delay of the propagation path from the BS to the IO plus from the IO to the MT together is larger than the total path delay. Note that the distance of the cluster from BS/MT and the cluster delay are chosen from independent distribution functions. As long as there are no joint distribution functions of the inter cluster delay spread and the angular spreads defined this effect may happen but has no influence on the validity of the model. In [28] joint angular and delay statistics are proposed. This novel approach avoids negative cluster link delays. However, a negative cluster link delay is somehow non physical and can be avoided via replacing the

corresponding cluster.
For a better illustration of the idea of the twin clusters Figure 2 shows a simulation scenario which covers 4 twin clusters. Each cluster has the shape of an ellipsoid. The IOs are depicted as small spheres. Due to different angular spreads at the MT and the BS the corresponding twins of one cluster are scaled versions of each other. This is the same as in real life: if you look at a twin from another perspective it may look different. But the distribution of IOs inside the cluster remains the same, it is just distorted. The clusters are numbered from 1 to 4 and the cluster number 1 at the BS side corresponds to its twin at the MT side. Different clusters may overlap. Overlapping may occur between two clusters of one side or one BS and one MT cluster twin. In the given example in Figure 2 clusters 1 and 3 overlap at the MT side but do not overlap at the BS twin.

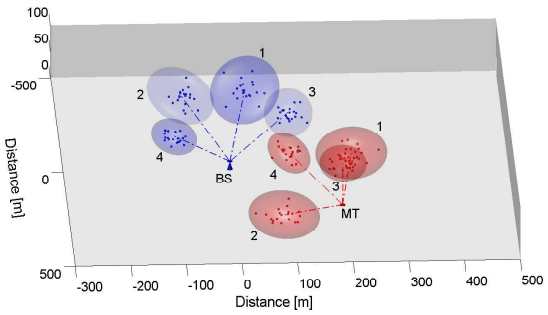

Figure 2. Example for the distribution of 4 twin clusters.

3. CLUSTER VISIBILITY

In contrast to the local cluster (i.e., the cluster around the MT) all other clusters are visible in certain regions only. In literature two differing approaches can be found: the placement of visibility regions [22] and a more stochastic approach using a birth-death process [29]. We have chosen the approach using visibility regions since it fits naturally into the geometric description of the simulation environment. The approach follows the method of COST 259 [30] and is repeated here for the convenience of the reader. The visibility regions are placed uniformly within the simulation area. Each visibility region corresponds to exactly one cluster and determines the position of the cluster. This may result in a huge set of clusters but only few of them are visible at a time and have to be considered for the computations. If the MT is in a visibility region, then a cluster is active and contributes to the impulse response; if the MT is outside the visibility region, the cluster does not contribute. The visibility region is characterized by R_{C}: size of the visibility region [m]. L_{C} : size of the transition region [m]. The size of such a visibility region depends on the simulation environment and is in the range of a few meters for pico-cells up to several hundred meters in rural areas. A smooth transition from a non-active to an active cluster is achieved by scaling the path gain of the cluster by a factor A_m^2. The transition function used is

$$A_m\left(\bar{r}_{MT}\right) = \frac{1}{2} - \frac{1}{\pi}\arctan\left(\frac{2\sqrt{2}y}{\sqrt{\lambda L_C}}\right) \tag{11}$$

with

$$y = L_C + \left|\bar{r}_{MT} - \bar{r}_m\right| - R_C. \tag{12}$$

where $\bar{r}_m$ is the center of the circular visibility area and λ is the wavelength. Furthermore, the visibility region is characterized by the probability density function of its location which depends on the distance between the visibility region and the BS. In order to give a constant expectation for the number of clusters that equals N_{C}, the area density of the visibility regions needs to be [27]

$$\rho_C = \frac{N_{\mathrm{C}} - 1}{\pi\left(R_{\mathrm{C}} - L_{\mathrm{C}}\right)^2} \quad \left[m^{-2}\right]. \tag{13}$$

ρ_C denotes the probability of a cluster center at any position of the simulation area. If R_{C} increases the total number of clusters needed for a scenario decreases.
The position of the cluster belonging to one visibility region is discussed below. The positions of the clusters should be fixed only once the MT enters a visibility region. Note that the resulting cluster is fixed in space and stays fixed as long as it is visible.
To combine the idea of visibility regions with the MT position dependent distribution of clusters each cluster has to belong to exactly one visibility region. Since the MT is moving through the visibility region but the cluster is fixed in space, the MT position is not taken into account for the cluster placement. Instead the center of the visibility region is used for the cluster placement. This approach even allows to place all the clusters before the start of the simulation which is a benefit for real time channel simulators since the real time computational effort is reduced.

4. MULTI-PATH COMPONENT DISTRIBUTION AND WEIGHTING

We have chosen an approach where small scale effects are separated from large scale effects and the individual parameters represent the structure of the model based on clusters and MPCs:

$$A_{\mathrm{s}} = P_{\mathrm{cl}} A_{\mathrm{MPC,s}}, \tag{14}$$

where P_{cl} denotes the attenuation coefficient of the whole cluster cl which allows for easy inter-cluster power adjustment. The attenuation of the single MPCs $A_{\mathrm{MPC,s}}$ influences the intra-cluster power delay profile and angular spreads and is discussed in detail in Section 4. The goal of the MPC placement and weighting is to achieve predefined angular-delay power-spectra (ADPS) for each cluster. Such spectra are, for example, defined in COST 259 and COST 273. The intra-cluster delay spread is defined there as exponentially decaying and the azimuth-spread has a double-sided Laplacian shape in [22]. In [31] the von Mises distribution is proposed for the placement of

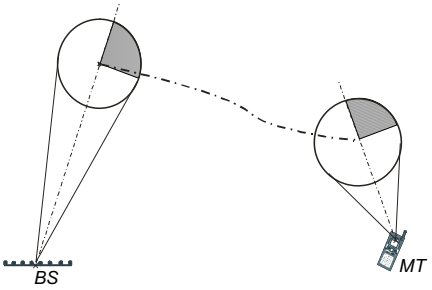

Figure 3. The rotation of the twin cluster at the MT and the BS side.

IOs inside a cluster instead of defining the intra-cluster angular and delay spread[2]. For our model the placement of the IOs inside the cluster follows a specific rule to ensure the predefined size of angular and delay spread. First, IOs are distributed according to a three-dimensional Gaussian distribution with variance $\sigma = 1$ inside a sphere

$$\overrightarrow{r} = \mathcal{N}\left(0, \begin{pmatrix} 1 & 0 & 0 \\ 0 & 1 & 0 \\ 0 & 0 & 1 \end{pmatrix}\right), \tag{15}$$

where $\mathcal{N}$ denotes a Gaussian distribution. This distribution of IOs is then transformed separately to the BS-side cluster and the MT-side cluster by

$$\overrightarrow{r}^{\,\mathrm{BS}}_{\mathrm{C,IO}} = \overrightarrow{r} \begin{pmatrix} d_{\mathrm{C}} \\ d_{\mathrm{C}} \\ h^{\mathrm{BS}}_{\mathrm{C}} \end{pmatrix} \mathrm{T}(\phi_{\mathrm{BS}}, \theta_{\mathrm{BS}}), \tag{16}$$

$$\overrightarrow{r}^{\,\mathrm{MT}}_{\mathrm{C,IO}} = \overrightarrow{r} \begin{pmatrix} d_{\mathrm{C}} \\ d_{\mathrm{C}} \\ h^{\mathrm{MT}}_{\mathrm{C}} \end{pmatrix} \mathrm{T}(\phi_{\mathrm{MT}}, \theta_{\mathrm{MT}}), \tag{17}$$

where T denotes the rotation matrix in space

$$\mathrm{T}(\phi, \theta) = \begin{pmatrix} \cos(\phi)\cos(\theta) & -\sin(\phi) & \cos(\phi)\sin(\theta) \\ \sin(\phi)\cos(\theta) & \cos(\phi) & \sin(\phi)\cos(\theta) \\ -\sin(\theta) & 0 & \cos(\theta) \end{pmatrix} \tag{18}$$

The rotation of the cluster is also depicted in Figure 3. This approach differs slightly from the COST 273 approach where an additional rotation of the MPCs at the MT side was proposed. It turned out that this additional rotation is not necessary for realistic PDPs.

5. IMPLEMENTATION OF THE MODEL

To exemplify the description of the model given in this paper and to aid further developments in the field, a Matlab implementation of the model is published under the GNU public license agreement. The source code can be downloaded from *www.ftw.at/cost273/*. It contains the twin clusters as part of the COST 273 MIMO channel model where the twin clusters were first introduced. The novel concept of twin-clusters is based on measurement evaluations and allows the usage of the model for several environment. As an example, a parameter set for a large urban macro cellular environment is given in Table 2. The parameter set is based on the COST 273 large urban macrocell scenario. However, our model only needs a subset of parameters of the comprehensive COST 273 model.

[2]For the IO placement the shape of the von Mises distribution is close to the shape of a truncated Gaussian distribution but easier to compute.

6. RESULTS

All the results of this section are based on the publicly available implementation of the model (see Section 5). The parameters of the large urban macrocell scenario (Table 2)were chosen. The COST 273 LUM scenario includes a local cluster around the MT. This cluster can be modelled using the twin cluster approach by placing both twins above each other at the position of the MT. The additional cluster link delay $\tau_{C,link}$ has to be set to zero for this cluster. The size of the cluster is determined by its angular spread as seen from the BS. All other clusters are placed according to the standard rules for placing twin clusters (see Section 2)

The transmit and receive side are using uniform linear arrays (ULA) with a spacing of $\lambda/2$. The characteristic of all antennas is isotropic. Furthermore a UMTS system with a center frequency of 2 GHz and a bandwidth of 5 MHz is assumed.

In Figure 4 the receive power levels of the first two Tx and Rx antennas of a 4x4 system with an antenna spacing of half a wavelength are shown. The signals show the typical small scale fading due to the multi path propagation with some deep fading dips. The resulting MIMO capacity is given in Figure 5. In addition to the standard antenna spacing of $\lambda/2$ we have also computed the capacity for an antenna spacing of $\lambda/10$, 5λ, and 15λ. As expected, the capacity increases for larger antenna spacings. For comparison the capacity of the i.i.d. channel is shown as well. Finally Figure 6 shows the Doppler spectrum of a single realization of the channel and the average Doppler spectrum averaged over 500 realizations of the channel. The speed of the MT was chosen at $v_{\mathrm{MT}} = 50$ m/s resulting in maximum Doppler shifts of $\nu_{\mathrm{D}} = \pm v_{\mathrm{MT}} \frac{f_c}{c_0} = \pm 333$ Hz. The average Doppler spectrum shows the classical 'bath-tube' effect of the well known Jake's spectrum [33]. It is slightly flatter since the channel model takes the elevation into account and is therefore not a 2-d model which is a precondition for obtaining the Jake's Doppler spectrum.

7. CONCLUSIONS

We are proposing a new way of modelling multiple interactions of multipath components with IOs between transmitter and receivers. The model is based on the concept of twin clusters that allow an independent adjustment of DoAs, DoDs, and delays, possibly based on measurement results. The model is therefore well suited for MIMO

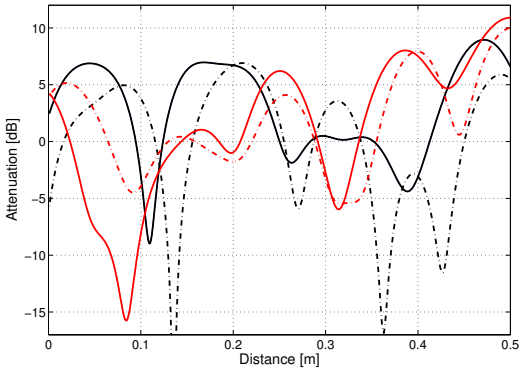

Figure 4. The receive power of the first 2 Rx and Tx antennas of a $4x4$ *MIMO system. Curves using the first Tx antenna are plotted in red and for the second Tx antenna in black. The solid lines denote for the first Rx antenna whereas the dash-dotted lines correspond to the second Rx antenna.*

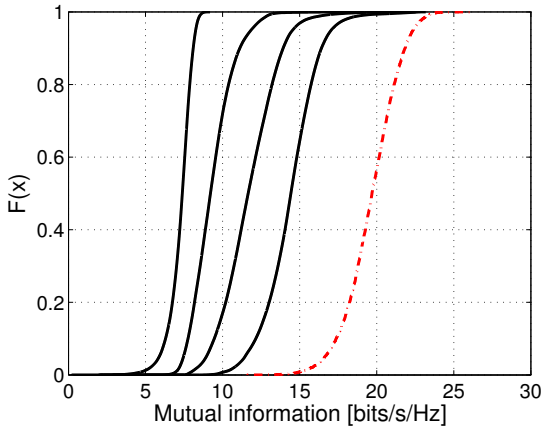

Figure 5. The MIMO capacity of a $4x4$ *MIMO system with antenna spacings of* 0.1*,* 0.5*,* 5*, and* 15λ*. For comparison the capacity of an i.i.d. channel is shown (red, dash-dotted line).*

channels.
The concept of the model allows for easy adaptation to several environments. Local clusters and far single interacting clusters, as e.g. in COST 259, can be modelled as special cases of the twin-cluster concept. In both cases the BS cluster twin and the MT cluster twin have to be placed on top of each other and the cluster link delay is set to zero.
The results show a very realistic behavior of our channel model. Properties of the wireless MIMO channel like the Doppler shift of the MPCs are inherently given by the model due to its geometry based design. The achieved MIMO capacity strongly depends on the antenna spacing but also on the environmental parameters like number of clusters and angular spreads.

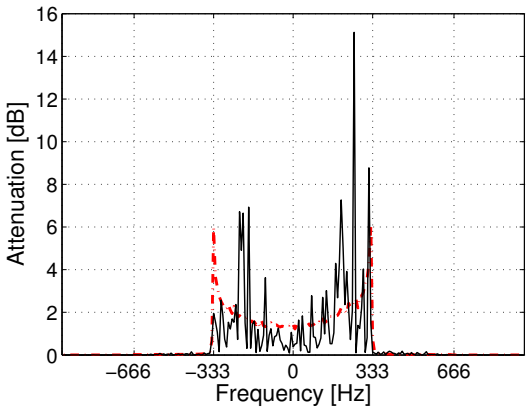

Figure 6. The Doppler spectrum of a single realization of the channel (black curve) and the Doppler spectrum averaged over 500 realizations (red, dash-dotted line).

ACKNOWLEDGMENT

The work was carried out within the NEWCOM Network of Excellence in Wireless Communications funded through the EC 6th Framework Programme.
The model was implemented within the ftw. project C9 "MIMO-UMTS for future packet services" together with Infineon Technologies, ARC Seibersdorf research, and Vienna University of Technology.
Research reported here was also supported by the Kplus program.

REFERENCES

1. J. H. Winters, "On the capacity of radio communications systems with diversity in Rayleigh fading environments," *IEEE J. Selected Areas Comm.*, vol. 5, pp. 871–878, June 1987.

2. G. J. Foschini and M. J. Gans, "On limits of wireless communications in a fading environment when using multiple antennas," *Wireless Personal Communications*, vol. 6, pp. 311–335, 1998.

3. G. J. Foschini, "Layered space-time architecture for wireless communication in a fading environment when using multi-element antennas," *Bell Labs Tech. J.*, vol. Autumn 1996, pp. 41–59, 1996.

4. V. V. Tarokh, H. Jafarkhani, and A. R. Calderbank, "Space-time block codes from orthogonal designs," *IEEE Trans. Information Theory*, vol. 45, pp. 1456–1467, 1999.

5. I. P802.11n/D1.0, "Draft amendment to Wireless LAN media access control (MAC) and physical layer (PHY) specifications: Enhancements for higher throughput," Tech. Rep., March 2006.

6. M. Steinbauer, A. F. Molisch, and E. Bonek, "The double-directional radio channel," *IEEE Antennas*

and Propagation Magazine, vol. 43, pp. 51–63, August 2001.

7. A. F. Molisch, *Wireless Communications*. IEEE Press Wiley, 2005.

8. W. C. Y. Lee, "Effects on correlation between two mobile radio base-station antennas," *IEEE Trans. Comm.*, vol. 21, pp. 1214–1224, 1973.

9. P. Petrus, J. H. Reed, and T. S. Rappaport, "Geometrical-based statistical macrocell channel model for mobile environments," *IEEE Trans. Communications*, vol. 50, pp. 495 –502, 2002.

10. J. J. Blanz and P. Jung, "A flexibly configurable spatial model for mobile radio channels," *IEEE Trans. Comm. 46*, pp. 367–371, 1998.

11. O. Norklit and J. B. Andersen, "Diffuse channel model and experimental results for array antennas in mobile environments," *IEEE Trans. Antennas and Propagation*, vol. 46, pp. 834 –840, 1998, similar to GSCM.

12. J. Fuhl, A. F. Molisch, and E. Bonek, "Unified channel model for mobile radio systems with smart antennas," *IEE Proc. Radar, Sonar and Navigation*, vol. 145, pp. 32–41, 1998.

13. A. Abdi and M. Kaveh, "A space-time correlation model for multielement antenna systems in mobile fading channels," *IEEE J. Selected Areas Comm.*, vol. 20, pp. 550–560, 2002.

14. M. Steinbauer and A. F. Molisch (eds.), "Directional channel models," in *Flexible Personalized Wireless Communications, L. Correia (ed.)*. J. Wiley, U.K., 2001, pp. 132–193.

15. A. Molisch, J. Laurila, and A. Kuchar, "Geometry-base stochastic model for mobile radio channels with directional component," *Proc. 2nd Intelligent Antenna Symp., Univ. Surrey*, 1998.

16. D. Gesbert, H. Boelcskei, and A. Paulraj, "Outdoor MIMO wireless channels: Models and performance prediction," *IEEE Trans. Comm.*, vol. 50, pp. 1926–1934, 2002.

17. A. F. Molisch, "A generic model for the mimo wireless propagation channel," *IEEE Proc. Signal Proc.*, pp. 61–71, 2004.

18. A. F. Molisch and H. Hofstetter, *Towards Mobile Broadband Multimedia Networks, COST 273 final report*, L. Correia, Ed. Elsevier Science Publishers B. V., 2006.

19. N. Czink, P. Cera, J. Salo, E. Bonek, J. Nuutinen, and J. Ylitalo, "A framework for automatic clustering of parametric mimo channel data including path powers," in *IEEE Vehicular Technology Conference 2006 Fall*, Montreal, Canada, 2006.

20. S. Wyne, N. Czink, J. Karedal, P. Almers, F. Tufvesson, and A. Molisch, "A cluster-based analysis of outdoor-to-indoor office mimo measurements at 5.2 ghz," in *IEEE Vehicular Technology Conference 2006 Fall*, Montreal, Canada, 2006.

21. L. Correia, Ed., *Towards Mobile Broadband Multimedia Networks*. Elsevier Science Publishers B. V., 2006.

22. ——, *Wireless Flexible Personalised Communications*. John Wiley & Sons, Ltd., 2001.

23. J. Blanz and P. Jung, "A flexibly configurable spatial model for mobile radio channels," *IEEE-Comm*, pp. 367–371, March 1998.

24. A. Molisch, A. Kuchar, J. Laurila, K. Hugl, and R. Schmalenberger, "Geometry-based directional model for mobile channels - principles and implementation," *ETT*, pp. 351–359, 2003.

25. T. Svantesson, "A double-bounce channel model for multi-polarized mimo systems," in *Vehicular Technology Conference IEEE 56th, Proceedings of*, vol. 2, Espoo, Finland, Sept. 2002, pp. 691–695.

26. A. Molisch, "A generic model for mimo wireless propagation channels in macro- and microcells," *IEEE-SP*, pp. 61–71, January 2004.

27. H. Asplund, A. A. Glazunov, A. F. Molisch, K. I. Pedersen, and M. Steinbauer, "The cost 259 directional channel model ii. macrocells," *IEEE Trans. Wireless Comm.*, p. submitted.

28. N. Czink, E. Bonek1, L. Hentil, P. Kyösti, J. Nuutinen, and J. Ylitalo, "The interdependence of cluster paramteres in mimo channel modeling," in *European Conference on Antennas and Propagation, Proceedings of*, Nice, France, Nov. 2006, p. to be published.

29. T. Zwick, C. Fischer, and W. Wiesbeck, "A stochastic multipath channel model including path directions for indoor environments," *Selected Areas in Communications, IEEE Journal on*, pp. 1178–1192, aug 2002.

30. A. Molisch, H. Asplund, R. Heddergott, M. Steinbauer, and T. Zwick, "The cost 259 directional channel model i. philosophy and general aspects," *IEEE Trans. Wireless Comm.*, p. in press.

31. X. Yin, T. Pedersen, N. Czink, and B. Fleury, "Parametric characterization and estimation of bi-azimuth dispersion of path components," in *Proc. SPAWC IEEE Workshop*, Cannes, France, 2006.

32. U. Trautwein, G. Sommerkorn, C. Schneider, and R. S. Thomä, "Measurement and analysis of mimo channels in public access scenarios at 5.2 ghz." in *Proc. WPMC Wireless Pers. Multimedia Commun.*, Aalborg, Denmark, 2005.

33. W. Jakes, *Microwave Mobile Communications*. New York: John Wiley, 1974.

$A_{VV,s}$	Attenuation of the vertical co-polarized path component of path s
$A_{VH,s}$	Attenuation of the cross-polarized part of the s^{th} path (from V to H)
$A_{HH,s}$	Attenuation of the horizontal co-polarized path component of path s
$A_{HV,s}$	Attenuation of the cross-polarized part of the s^{th} path (from H to V)
τ_s	Path delay of path s
$\phi_{DoD,s}$	Direction of Departure in Azimuth of path s
$\theta_{DoD,s}$	Direction of Departure in Elevation of path s
$\phi_{DoA,s}$	Direction of Arrival in Azimuth of path s
$\theta_{DoA,s}$	Direction of Arrival in Elevation of path s

Table 1. Set of parameters defining one MPC.

Parameter	**Value**	**Comments, including references**
f_c [Hz]	900 MHz - 2 GHz	2 GHz is typical because of UMTS
h_{BS} [m]	50	from COST 259
h_{MS} [m]	1.5	pedestrian walking
$\overrightarrow{r}_{\text{BS}}$ [m]	(0,0,0)	origin of coordinate system
$\overrightarrow{r}_{\text{MS}}$ [m]	uniform distributed in cell area	
cell radius [m]	1000	
Visibility region		
R_{C} [m]	100	from COST 259
L_{C} [m]	20	from COST 259
Average number of clusters N_{C}	2.18	from COST 259 (BU)
Number of MPCs per cluster N_{MPC}	20	from [32]
Cluster delay $\mathcal{F}(\tau_{\text{C}})$	0.5 / 3	
Inter cluster angular spread at BS		
$\mathcal{F}(\Phi_{\text{BS}})$ $[^o]$	U$[0, 360[$	
$\mathcal{F}(\Theta_{\text{BS}})$ $[^o]$	U$[-10, 0]$	
Inter cluster angular spread at MT		
$\mathcal{F}(\Phi_{\text{MT}})$ $[^o]$	U$[0, 360[$	
$\mathcal{F}(\Theta_{\text{MT}})$ $[^o]$	U$[0, 45]$	
Intra cluster delay spread		
μ_τ [μs] / σ_τ [dB]	0.4/3	
Intra cluster angular spread at BS		
$\mathcal{F}(\Phi_{\text{BS}})$: $\mu_{\varphi\text{BS}}$ [$^\circ$] / $\sigma_{\varphi\text{BS}}$ [dB]	0.81/0.34	from 3GPP;
$\mathcal{F}(\Theta_{\text{BS}})$: $\mu_{\vartheta\text{BS}}$ [$^\circ$] / $\sigma_{\vartheta\text{BS}}$ [dB]	0.5/3	from COST 259
Intra cluster angular spread at MT		
$\mathcal{F}(\Phi_{\text{BS}})$: $\mu_{\varphi\text{MT}}$ [$^\circ$] / $\sigma_{\varphi\text{MT}}$ [dB]	35 / 0	from 3GPP
$\mathcal{F}(\Theta_{\text{BS}})$: $\mu_{\vartheta\text{MT}}$ [$^\circ$] / $\sigma_{\vartheta\text{MT}}$ [dB]	10 / 3	

Table 2. Parameter set for a large urban macro cell environment [21].